ACS OMEGA

http://pubs.acs.org/journal/acsodf

Article

An Efficient Cross-Linked Phosphorus-Free Flame Retardant for Epoxy Resins

Rui Wang, Penglun Zheng,* Junwei Li, Jichang Sun, Huaiyin Liu, Xue Li,* and Quanyi Liu*

Cite This: *ACS Omega* 2022, 7, 37170−37179

Read Online

ACCESS | Metrics & More | Article Recommendations

ABSTRACT: Epoxy resins (EPs) have been widely used due to their great physical and chemical properties, but their poor flame retardancy limits their further application. In this work, we synthesized a flame retardant containing nitrile groups and a double bond to improve the flame retardancy of EPs. In this way, multiple cross-linking reactions can occur in the EPs to confer better flame retardancy by a simple heat treatment. The UL-94 vertical combustion test, CCT, and limiting oxygen index (LOI) test were used to characterize the flame retardant properties of the cross-linked flame retardant; the results show that with the 10 wt % addition of cross-linked flame retardant, the thermosets can pass the UL-94 V-0 rating. Meanwhile, the contents reached 20 wt %, and the peak heat release rate decreased 40% compared with neat EP.

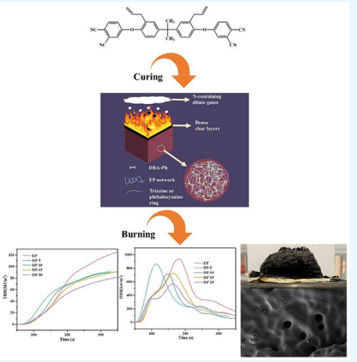

1. INTRODUCTION

Due to their comprehensive performances in physical, electrical, and chemical processing, epoxy resins (EPs) are extensively applied in many engineering fields and our daily life.[1−6] But it cannot be ignored that they are highly flammable in the air.[7−9] In past decades, researchers have put a lot of effort into flame-retardant EPs.[10−12] Among all of the procedures taken, from the perspective of environment protection, halogen-free flame retardants catch the most attention.[13−17] And since the organic flame retardants can be better dispersed in an EP matrix and the structure can be designed in several different ways, they have become the hottest topic in the EP flame retardants area.[18−20] Phosphorus-containing flame retardants have good flame retardancy, but the phosphorus-containing flame retardants face secondary pollution and migration during practical applications.[21−24] So, phosphorus-free organic flame retardants are the latest trend in developing new flame retardants for the aim of improving the safety of the flame retardants.[25,26]

Recently, researchers have found that when the flame retardants get cross-linked inside the EP matrix, the flame-retardant performances are improved. Jin et al. synthesized a flame retardant which contains two C═C bonds. They can get cross-linked during the curing process of EP, and the results showed that while the addition amount was only 4 wt %, the EP thermosets can pass the UL-94 V-0 rate and get a limiting oxygen index (LOI) value of 35.6%.[27] Peng et al. designed phthalonitrile-group-containing compounds and treated the EP thermoset with another thermal procedure to make the flame retardant cross-link, and the flame-retardant cross-linked EP thermosets have an LOI value of 46.2% and pass the UL-94 V-0 rate.[2]

The above flame retardants are all phosphorus-containing flame retardants, inspired by the cross-linking strategy, and in order to reduce the secondary pollution caused by phosphorus-containing flame retardants, phosphorus-free and halogen-free flame retardants have been applied in this work. In this work, we introduce the nitrile groups and double bond into the flame retardant; a multiple cross-linking reaction can occur by a simple heat treatment in EPs to further endow them with flame-retardant properties.[28,29] The UL-94 vertical combustion test, CCT, and limiting oxygen index (LOI) test were used to detect the flame-retardant properties of the cross-linked flame retardant; the results show that with 10 wt % content of cross-linked flame retardant, the thermosets can pass the UL-94 V-0 rating. Meanwhile, the contents reached 20 wt % and the peak heat release rate decreased for 40% compared with neat EP.

2. EXPERIMENTAL SECTION

2.1. Materials. Diglycidyl ether of biphenol A (DGEBA, commercial code: E-51, epoxide value of 0.51 mol/100 g) was purchased from Shandong Jiaying Chemical Technology Co., Ltd., China. The 4,4′-diaminodiphenylsulphone (DDS) and

Received: May 21, 2022
Accepted: October 3, 2022
Published: October 10, 2022

DBA were purchased from Shanghai Yien Chemical Technology Co., Ltd., China. 4-NPh was purchased from Adams. Ethanol, anhydrous potassium carbonate (K_2CO_3), and dimethyl sulfoxide (DMSO) were purchased from Chengdu Chron Chemicals Co., Ltd., China.

2.2. Preparation of the DBA-Ph. First, 15.4 g of DBA and 15 g of K_2CO_3 were put into a 250 mL three-neck flask; then 100 mL DMSO was added. The mixed solution was heaed to 75 °C and the condensation reflux stirred. After 4 h, 17.3 g of 4-NPh was added; the reaction temperature was kept at 75 °C for another 3 h. The solution was then added into water. There, the solid separated out, and after filtration, the received solid was put into ethanol, smashed to powder, and washed several times with ethanol until the ethanol was colorless. Finally, the light yellow powder DBA-Ph[30] was obtained after the ethanol was removed by putting it in a 60 °C oven for 24 h (as shown in Scheme. 1).

Scheme 1. Synthesis Routine of DBA-Ph

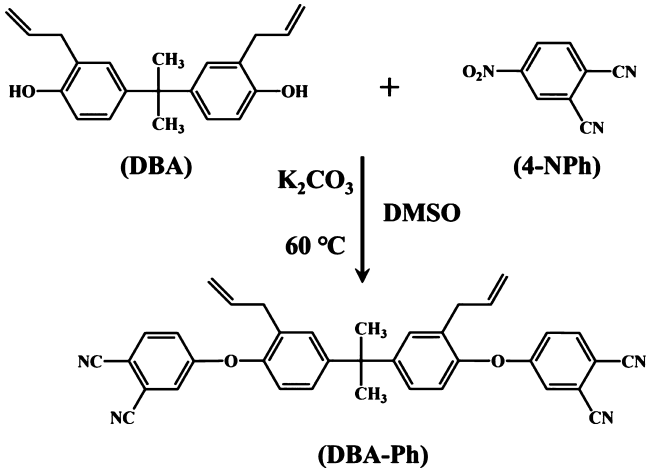

2.3. Preparation of the EP Thermosets. The E51 and DDS were put together and stirred under 120 °C until the DDS was fully dissolved, then the mixed solution along with DBA-Ph would go through another 30 min stirring. After that, in a vacuum oven, the mixed liquid was poured into the molds, which had been already warmed up to 120 °C; then the oven was vacuumed for 30 min to ensure that there were no bubbles inside the samples. Finally, a 4 h at 190 °C procedure was needed to make the EP mixture fully cured, and for DBA-Ph to cross-link, another heat treatment was needed. There were three different temperatures (210 °C, 230 °C, 250 °C), and each temperature was held for 2 h. And, the contents of E51, DDS, and DBA-Ph are shown in Table 1.

2.4. Measurements. The structure of the compounds needed to be confirmed; the tools chosen for detecting them were Fourier Transform Infrared (FTIR) and ^{1}H NMR spectra, which were collected on a PerkinElmer Spectrum Two instrument and a Bruker Avance III-400 NMR spectrometer.

Table 1. E51, DDS, and DBA-Ph Contents of EP Thermosets

samples	E-51 (wt %)	DDS (wt %)	DBA-Ph (wt %)
EP	76.9	23.1	0
DP-5	73.1	21.9	5
DP-10	69.2	20.8	10
DP-15	65.4	19.6	15
DP-20	61.5	18.5	20

The curing behaviors of the samples with DBA-Ph would show some difference compared with the neat ones, so a PerkinElmer DSC 4000 instrument was used to find out these differences.

The decomposition features of the samples were observed via a thermogravimetric analyzer (PerkinElmer TGA 4000). The results were put into thermogravimetric analysis (TG) spectra.

A JF-3 oxygen index apparatus (Nanjing Jiangning Instrument Factory, China) and a CZF-2 burning tester (Nanjing Jiangning Instrument Factory, China) were used to measure the flame-retardant properties of DBA-Ph through testing the epoxy thermosets with and without it. And the properties showed that, when they were ignited, they were also measured via a cone calorimeter test (CCT)

The dynamic mechanical properties and the cross-linking degree can be determined using a DMA 850 (TA Instrument, USA). The dynamic mechanical analysis (DMA) results could tell the glass transition temperature (Tg) of the EP thermosets, which was the key parameter of the dynamic mechanical properties and the cross-linking degree.

The flame-retardant mechanisms were another important aspect needed to be found; in the gas phase, the thermal decomposition products could be collected and identified through FTIR, so a PerkinElmer Spectrum Two instrument was attached with a PerkinElmer TGA 4000 to gather the FTIR spectra of the gases. For the condensed phase, a Hitachi S-4800 scanning electron microscope (SEM) was applied to observe the microstructure of the residue char after CCT tests, and a LabRAM-HR Evolution Raman Microprobe (France) was used to analyze the toughness of the residue char through the graphitization degree.

3. RESULTS AND DISCUSSION

3.1. Characterization of DBA-Ph. The FTIR spectrum of DBA-Ph is shown in Figure 1a. From the FTIR spectrum of DBA-Ph, the peaks at 3082 and 2974 cm^{-1} corresponded to the C−H bonds from =C−H and $-CH_3$; the characteristic peaks of allyl groups in the structure of DBA-Ph were shown at 1639 cm^{-1} and 841 cm^{-1} ($-CH{=}CH_2$) and 1411 cm^{-1} ($C{=}C{-}CH_2$). And the reaction between DBA and 4-NPh was proved by the appearance of the Ar−O−Ar at 1243 cm^{-1} and the maintenance of −CN at 2230 cm^{-1}. The FTIR results were strong evidence of the successful synthesis of DBA-Ph.

Furthermore, the ^{1}H NMR was also applied to characterize the chemical structure of DBA-Ph. As shown in Figure 1b, the corresponding peaks of the H atoms in DBA-Ph were marked in the spectrum. The hydrogen atoms (H) on allyl were observed at the peaks from 3.22 to 5.80 ppm. It was noticed that there was a high peak at 1.89 ppm; the methyl hydrogen atom (H) was detected and shown at this peak. In the NMR, the integral area ratios of these different kinds of H atoms are also consistent with the theoretical values, so the above NMR results provided more evidence for the successful synthesis of the DBA-Ph.

3.2. Further Treatment of EP. To make the C=C bonds and nitrile groups in the DBA-Ph structure completely cross-linked inside the EP matrix, a further thermal treating procedure was needed after the curing of the EP matrix. In

https://doi.org/10.1021/acsomega.2c03167
ACS Omega 2022, 7, 37170−37179

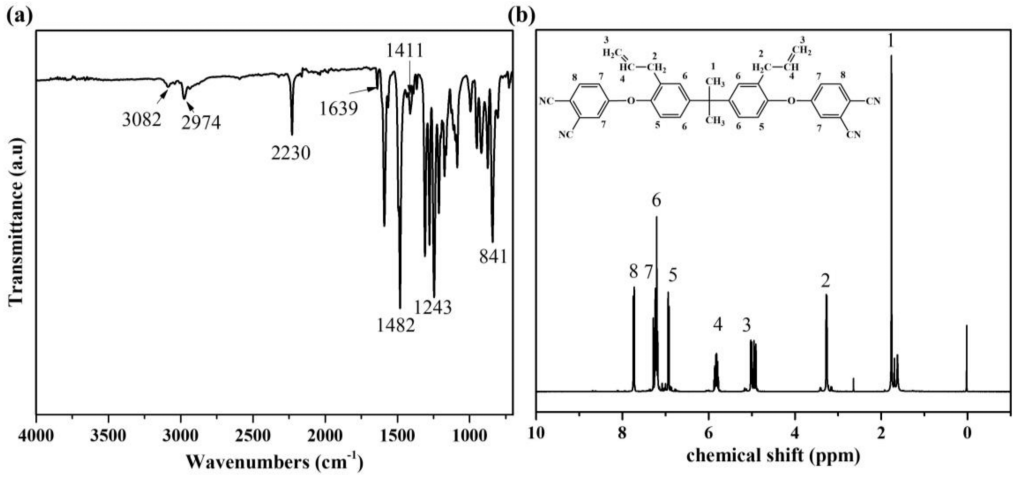

Figure 1. (a) FTIR spectrum of DBA-Ph and (b) ^{1}H NMR spectra of DBA-Ph.

order to determine the temperature of the thermal treating procedure, DSC tests of all of the prepolymers were applied. The DSC testing temperature range was 30 to 300 °C at a rate of 5 °C/min, as shown in Figure 2. All of the DSC curves were showing a broad peak; this is mainly attributed to the curing reaction of the EP. With the introduction of DBA-Ph, the exothermic peak temperature was increased. The above phenomenon indicated that with the increasing of DBA-Ph content, the density of the nitrile group could enable the cross-linking reaction to occur freely, so the high cross-linking reaction of the nitrile group in DBA-Ph caused the exothermic temperature to start to increase.[2,31] Another interesting phenomenon was that the samples with DBA-Ph all showed the trend of forming a double exothermic peak. That was the strong evidence of the multiple cross-linking reaction of DBA-Ph/EP. The TG curve was used to test the decomposition temperature of DPA-Ph/EP composites. From Figure 3a, the DBA-Ph/EP samples did not decompose until 291 °C, and the DBA-Ph started to decompose at 268 °C. Finally, the heat treatment chosen for DBA-Ph-doped EP composites was 210 °C, 230 °C, and 250 °C, each for 2 h.

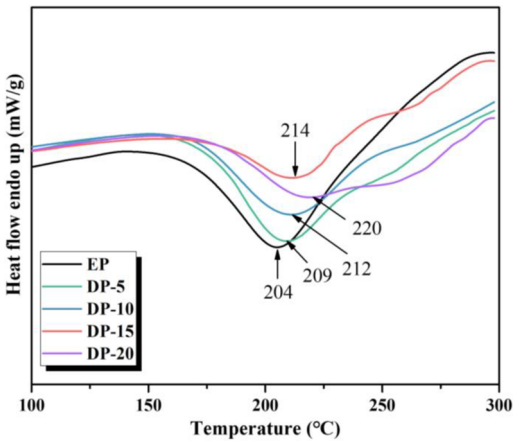

Figure 2. DSC curves of the prepolymers of EP and EP composites.

3.3. TG Analysis of EP Composites. TG tests of all of the EP samples and DBA-Ph were made to analyze the thermal properties of samples, as in Figure 3, and some parameters, $T_{5\%}$ (the temperature when the mass loss was at 5 wt %), T_{max} (temperature when the mass loss reached the top), D_{max} (the top point of the DTG curve), and Cr_{700} (the residue char weight content at 700 °C), in TG curves are shown in Table 2. The results showed that the DBA-Ph had great thermal stability. The mass loss did not exceed 5 wt % at temperatures

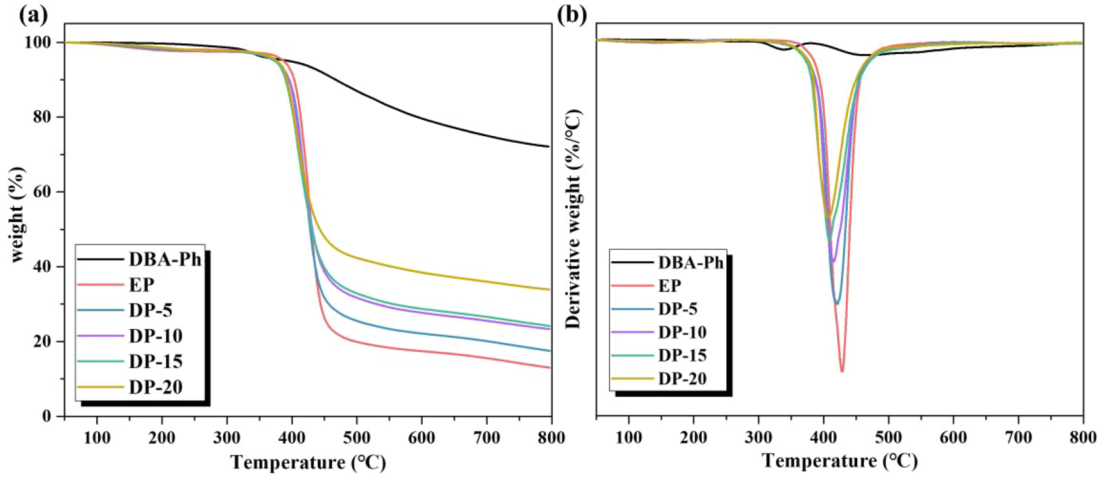

Figure 3. TG curves (a) and DTG curves (b).

https://doi.org/10.1021/acsomega.2c03167
ACS Omega 2022, 7, 37170−37179

Table 2. Key Parameters of the EP Samples in TG Analysis under N_2

samples	$T_{5\%}$ (°C)	T_{max} (°C)	D_{max} (%/°C)	Cr_{700} (%) theoretical value	Cr_{700} (%) actual value
DBA-Ph	396	462	−0.10		75.1
EP	386	427	−2.02		15.2
DP-5	374	420	−1.61	18.2	20.1
DP-10	375	415	−1.35	21.2	25.4
DP-15	373	408	−1.21	24.2	26.6
DP-20	376	407	−1.08	27.8	36.1

less than 396 °C, and while the DBA-Ph was introduced into EP, the $T_{5\%}$ instead got a decrease. It might be attribute to the fact that the addition of DBA-Ph would promote the decomposition of the EP. Furthermore, the introduction of DBA-Ph could efficiently lower D_{max} values, indicating that the DBA-Ph could prevent the decomposition of the EP composites at a lower degree, but the T_{max} had also decreased with the increasing DBA-Ph content. The DBA-Ph have the catalysis effect for the decomposition of EP matrix at a lower temperature. The Cr_{700} showed in Table 2 exhibited that the DBA-Ph could promote the produce of residue char, more residue char content, better flame retardancy. In summary, with the incorporation of DBA-Ph, the EP composites showed a lower decomposition degree and more residue char.

3.4. DMA Tests of the Samples. The T_g value could be told from the peaks of the tan delta curves, which were obtained from the DMA tests, as shown in Figure 4. The T_g values could be used to characterize the mobility of the polymer segment under high temperature, which were influenced by the cross-linking density, packing, and entangled segment degree.[32] The T_g results showed that DP-5 has the highest T_g, and with the increasing DBA-Ph content, the T_g of DP-10 and DP-15 was decreased, but when the DBA-Ph content reached 20 wt %, the T_g in turn got a rise. Other important information was that the T_g of all of the modified EP samples was never lower than the neat one. The cross-linking density of the samples would be evaluated through the cross-linking reaction of DBA-Ph inside the EP matrix, so there was a clear rise for DP-5 in the T_g value, but the rigid groups in DBA-Ph had a negative effect on T_g with large molecular chains leading to a decrease in cross-link density.[33] Therefore, while the DBA-Ph content continued to rise, the negative effect of the rigid groups overcame the positive effect of the cross-linking density increase, so the T_g of DP-10 and DP-15 got a decrease instead. But when the DBA-Ph content reached 20 wt %, the positive effect again overcame the negative effect and made the T_g of the sample rise again. In summary, DBA-Ph had a positive effect of increasing the T_g of EP samples.

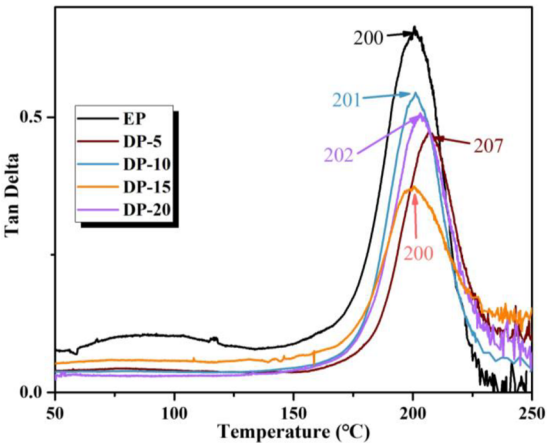

Figure 4. DMA curves of the samples.

As shown in Figure 5, the storage modulus of DP-20 possesses higher values than pure EPs. Generally, the storage modulus is related to the rigidity and cohesive energy density of the network. C≡N rigid bonds from DBA-Ph have been introduced into the EP matrix through physical mixing; meanwhile, multiple cross-linking reactions can occur in the EPs by a simple heat treatment. The storage modulus increased and the loss modulus decreased with the increasing content of flame retardants.

3.5. Evaluation of the Burning and Flame-Retardant Properties. The flame-retardant properties of the materials were evaluated by LOI tests and UL-94 vertical burning tests. As shown in Table 3, neat EP is highly flammable in air, and its LOI is only 22.4%. The digital photos shown in Figure 6 further confirmed this conclusion; it burns severely and drips with melt, not stopping until it burns out. And incorporating it with 5 wt % of DBA-Ph, the LOI value rose to 29.5%, which already makes DP-5 a flame-retardant material. When further increasing the contents of DBA-Ph, there was a slight increase in LOI value with every 5 wt % DBA-Ph content increase, and it finally reached an LOI value of 34.9% with the contents reaching 20 wt %. On the other hand, all samples reached UL-94 V-0 except the DP-5 thermosets.

As shown in Table 4 and Figure 7, the combustion properties of DP samples can be characterized by the results received from CCT. First, with the addition of DBA-Ph, the peak heat release rate (PHRR) value received from CCT was sharply decreased. The PHRR decreased to 60% in PHRR values for DP-20 compared to neat EP. THR results showed the same trend as the PHRR results; when DBA-Ph content reached 20 wt %, the THR value was decreased from 135.13 MJ/m^2 to around 83.87 MJ/m^2. The reduced values of THR and HRR indicate that the introduction of DBA-Ph imparts flame retardancy to epoxy thermosets. The average effective heat combustion (av-EHC) value usually indicated the degree of gas combustion during combustion in the gas phase.[34] And the av-EHC value showed almost the same trend with the THR value. This indicates that BA-Ph has a significant role in gas phase flame retardancy. It diluted oxygen and those combustible gases by producing noncombustible gases; the more compact residual char from the IPN structure will further reduce combustible and noncombustible gas leakage. A sharp decrease happened for the total smoke produced (TSP) and total smoke released (TSR) values of the DP samples compared with EP, and the total mass loss (TML) value exhibited a clearly downward trend. On the basis of these results, this indicated that cross-linked flame retardants can effectively improve the flame retardancy of EP. This is mainly attributed to the IPN structure improving the denseness of the residue char, which can obstruct the transfer of heat, thus improving fire safety.

3.6. Analysis in Condensed Phase. With the analysis of the values from CCT, it was found that when the DBA-Ph content increased, the residue char was also increased. Therefore, it is necessary to analyze the structure of the residual char. As shown in Figure 8, from the residue char

https://doi.org/10.1021/acsomega.2c03167
ACS Omega 2022, 7, 37170−37179

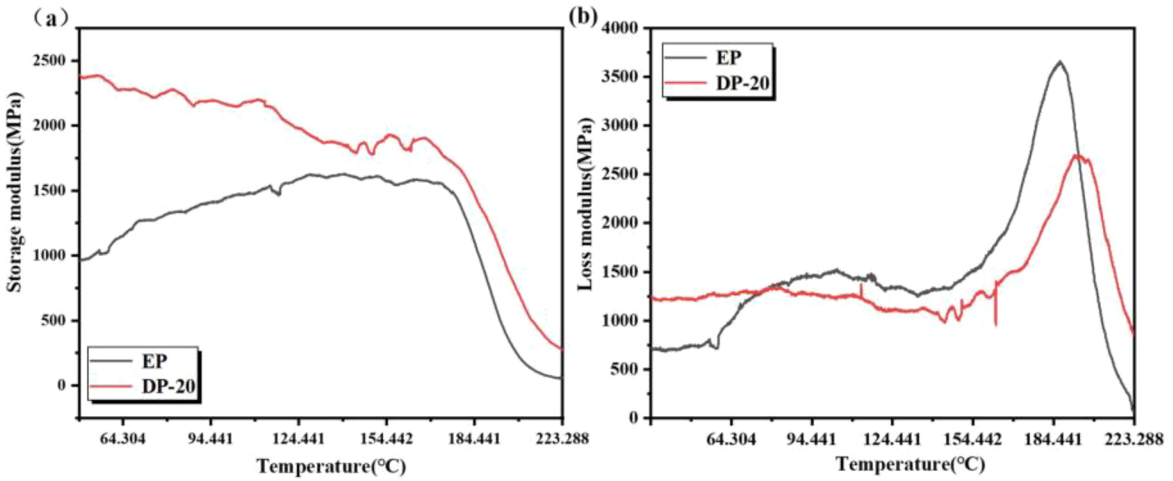

Figure 5. Modulus of the testing samples. (a) Storage modulus; (b) loss modulus.

Table 3. UL-94 Burning Tests and LOI Results of EP Samples

			UL-94 burning test			
samples	LOI (%)	t_1 (s)	t_2 (s)	dripping	rate	test times
EP	22.4	>100		yes	NR	5
DP-5	29.5	6 ± 2	2 ± 1	no	V-1	5
DP-10	32.9	4 ± 0.5	2 ± 0.5	no	V-0	5
DP-15	34.7	2 ± 0.5	1 ± 0.5	no	V-0	5
DP-20	34.9	1 ± 1	1 ± 0.5	no	V-0	5

photos obtained after CCT, with the increasing content of DBA-Ph, the macro-view of the residue char exhibited a clear trend that the char layers became more completed and more expanded. Complete and expanded residue char surely can hinder the heat diffusion and smoke leakage well. The residue char of DP-5 showed an incomplete status. And, the tin foil was burned through just like EP samples, but it still showed a better status than the char layers of EP. And when the content of DBA-Ph increased to 10 wt %, the tin foil could not be

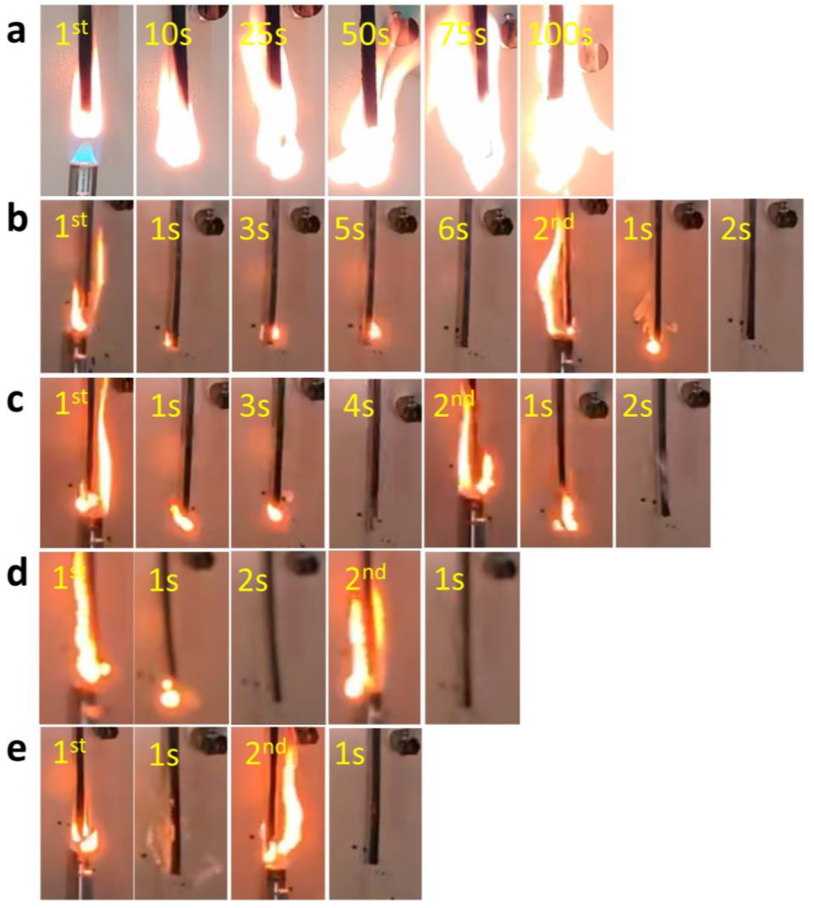

Figure 6. Digital photos in UL-94 vertical burning test. (a) EP, (b) DP-5, (c) DP-10, (d) DP-15, (e) DP-20.

https://doi.org/10.1021/acsomega.2c03167
ACS Omega 2022, 7, 37170−37179

Table 4. CCT Results of EP Samples

samples	TTI (s)	PHRR (kW/m^2)	THR (MJ/m^2)	av-EHC (MJ/kg)	TSP (m^2)	TSR (m^2/m^2)	TML (wt %)
EP	43 ± 3	1006.02 ± 25	135.13 ± 1.5	25.5	46.9	5305.4 ± 25	90.7
DP-5	40 ± 4	926.13 ± 12	92.65 ± 1.2	22.5	35.2	3980.8 ± 18	88.5
DP-10	45 ± 3	885.33 ± 14	90.94 ± 0.7	22.1	31.1	3521.5 ± 14	84.5
DP-15	48 ± 2	758.84 ± 10	94.78 ± 0.8	22.2	32.6	3688.9 ± 7	80.3
DP-20	42 ± 4	603.24 ± 18	83.87 ± 1.1	20.8	33.7	3808.8 ± 8	78.2

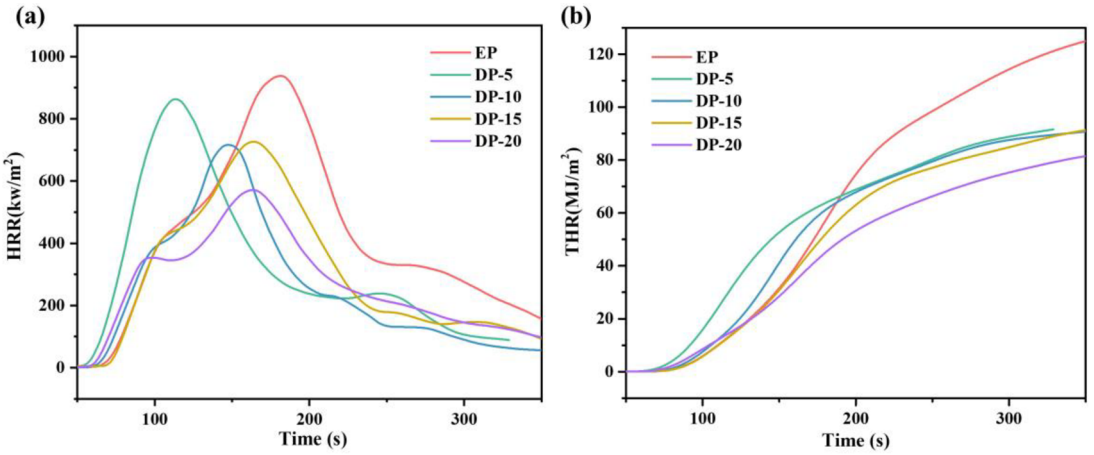

Figure 7. HRR (a) and THR (b) curves of EP thermosets.

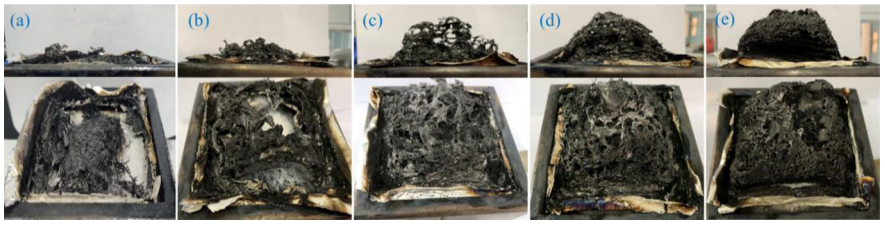

Figure 8. Digital photos after CCT. (a) EP, (b) DP-5, (c) DP-10, (d) DP-15, (e) DP-20.

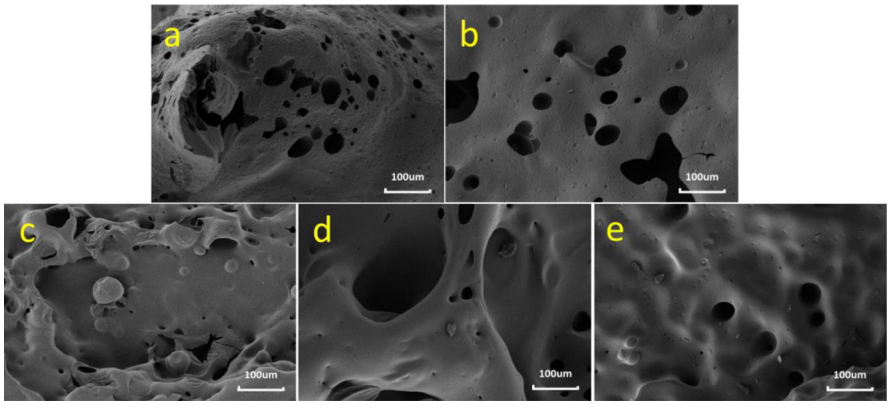

Figure 9. SEM images samples in Figure 8. (a) EP, (b) DP-5, (c) DP-10, (d) DP-15, (e) DP-20.

burned through anymore, and some big holes appeared. That was the evidence for the leakage of the smoke and heat. The smaller holes mean less leakage, so the more completed and expanded residue char had smaller holes, therefore showing a better heat and smoke barrier effect. There were already some extremely small holes on the surface of the DP-20 residue char. Then, the microview of the char layers is shown in Figure 9. The surface of the EP char layer had many holes, and some cracks were also observed. The DP-5 sample also had many holes and some cracks. More importantly, the morphology of those holes and cracks shown in these two charcoal layers indicated that the charcoal layer was thin because the holes and cracks were not three-dimensional. The charcoal layers of DP-10, DP-15, and DP-20 all were three-dimensional, which meant that the charcoal layer was thick. Furthermore, except for the holes, some bubbles were also shown in the surface of DP-10, DP-15, and DP-20, this phenomenon could prove that the char layer could hinder the heat and smoke from leaking.

https://doi.org/10.1021/acsomega.2c03167
ACS Omega 2022, 7, 37170−37179

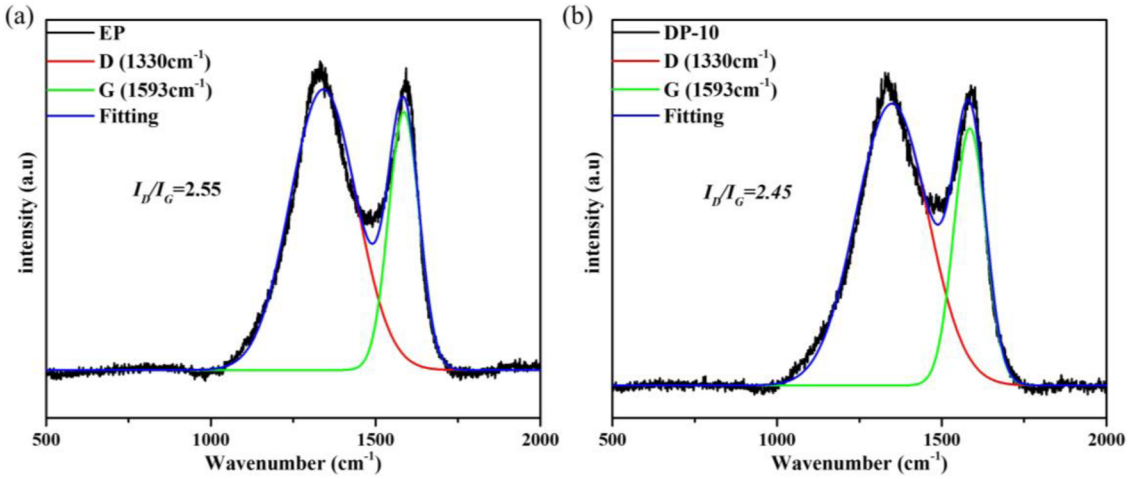

Figure 10. Raman spectra of the residue char. (a) EP and (b) DP-10.

Moreover, in order to prove that the greater the DBA-Ph content, the more complete and firm the char layer, Raman spectroscopy was used. In Figure 10, the I_D/I_G value of EP and DP-10 is showed, and the char layers with a better compactness and thermal stability would lower the I_D/I_G value.[35] The value clearly showed that DP-10 had higher compactness and thermal stability, which also could be interpreted as DBA-Ph having the ability to make the char layer become more completed and tougher, while it insulates the transfer of heat and thus exhibits excellent flame retardancy in the condensed phase.

3.7. Analysis in Gas Phase. The gas products of the EP composites when being heated could be characterized by the TG-FTIR. As shown in Figure 11a, the components of neat EP mainly contained hydrocarbons ($-CH_2$, $-CH_3$; 1251 and 3010 cm^{-1}) and H_2O at about 3580 cm^{-1}, carbon dioxide (2360 cm^{-1}), and aromatic compounds (805 and 1508 cm^{-1}); in addition, SO_2 was also found between 1300 and 1400 cm^{-1}.[36,37] And some new peaks were observed in Figure 11b; the peaks around 950 and 1580 cm^{-1} were referred to N-containing gases, including NH_3, NO, and NO_2.[38] These gases belonged to the inflammable gases; they could dilute O_2, flammable gases, and heat along with CO_2 and SO_2. Therefore, the diluted effect brought by these inflammable gases could make the EP samples have incomplete combustion. The peaks shown at around 2050 cm^{-1} could prove this, since the peaks belonged to CO, and the incomplete combustion of product CO_2 peaks in Figure 11b also weakened.

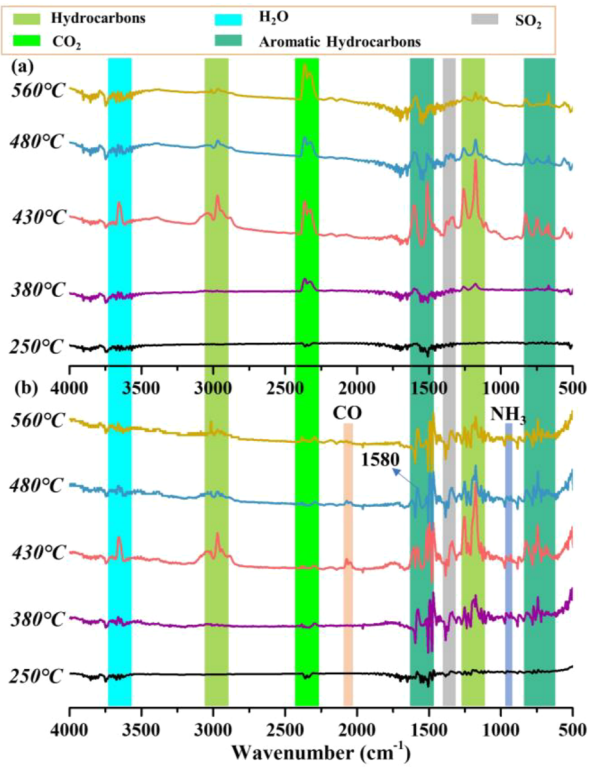

Figure 11. TG-FTIR spectra of the (a) EP and (b) DP-20.

To more deeply understand the pyrolysis behavior of the DBA-Ph/epoxy thermosets, the flame retardant was tested by Py-GC/MS; the spectra are shown in Figure 12. DBA-Ph was first decomposed into two parts; during this process, double bond and nitrile groups were generated. At the same time, the active hydrogen produced by decomposition promotes the cross-linking of the nitrile groups to form a denser cross-linked structure, thus producing a denser char layer. The proposed pyrolysis route obtained from the characteristic peaks is shown in Scheme. 2.

3.8. Flame-Retardant Mechanisms of DBA-Ph. After analyzing of the gas products in the condensed and gas phases of the burned EP thermosets, as shown in Figure 13, the DBA-Ph was clearly shown to have the flame-retardant effects in both the condensed phase and gas phase; the details are as follows. First, the generation of noncombustible gases in the gas phase can dilute combustible gases and O_2, thus inhibiting the continuation of gas-phase combustion. Meanwhile, in the condensed phase, the modified BA-Ph/EP samples can form a char layer with residual char structure on the surface of the combustible material, while the multiple cross-linked network structure enhances the denseness of the char layer. The dense char layer isolates the feedback of oxygen and combustion heat to the substrate, effectively suppressing the rise in material temperature, while lowering the thermal decomposition temperature of the material and reducing the release of combustible gases, thus functioning in the condensed phase.[39−43] In conclusion, the modified DBA-Ph/EP samples exhibited good flame retardant properties in both the gas and condensed phases.

https://doi.org/10.1021/acsomega.2c03167
ACS Omega 2022, 7, 37170−37179

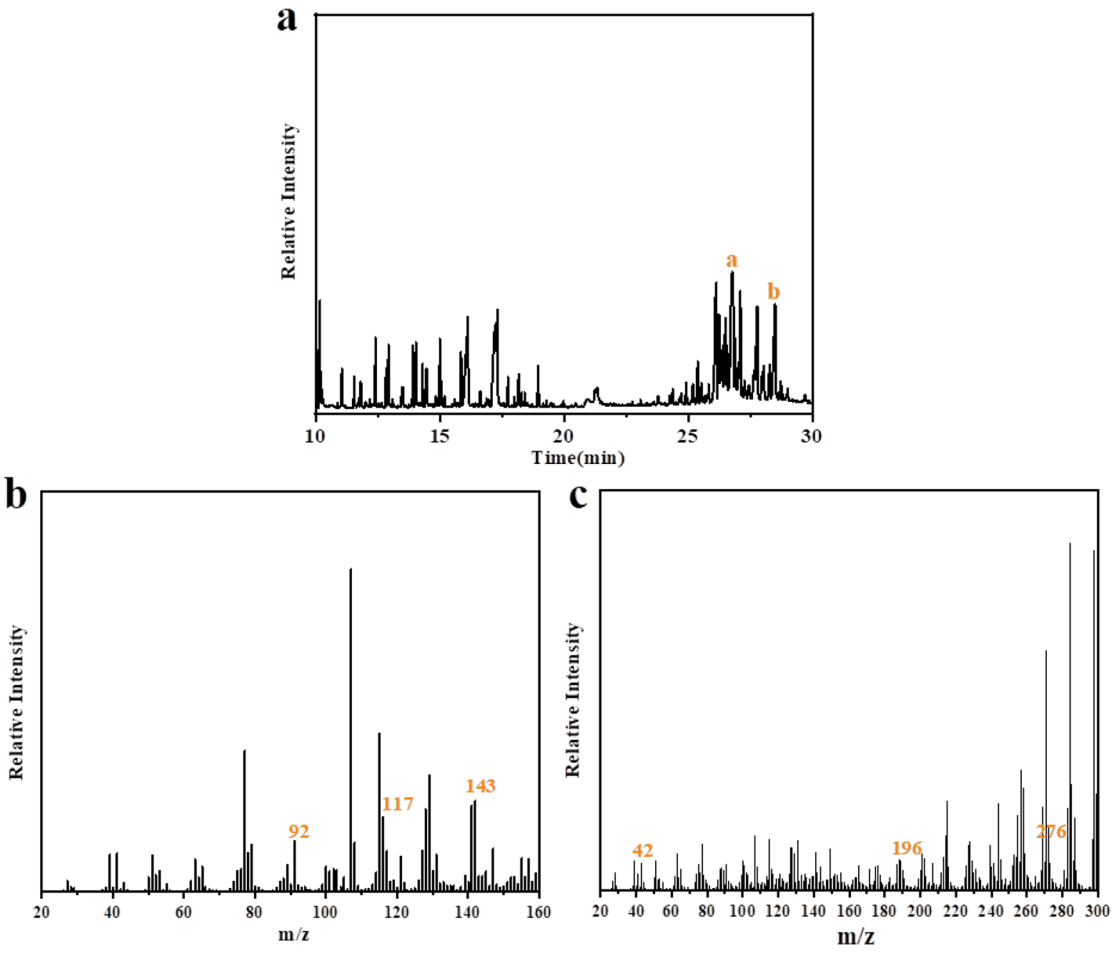

Figure 12. (a) Total ion chromatogram (TIC). (b, c) MS spectra of main pyrolysis products of DBA-Ph.

Scheme 2. Proposed Pyrolytic Route of DBA-Ph

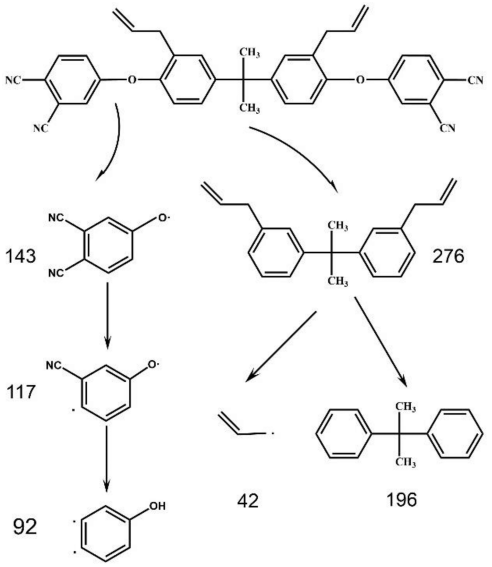

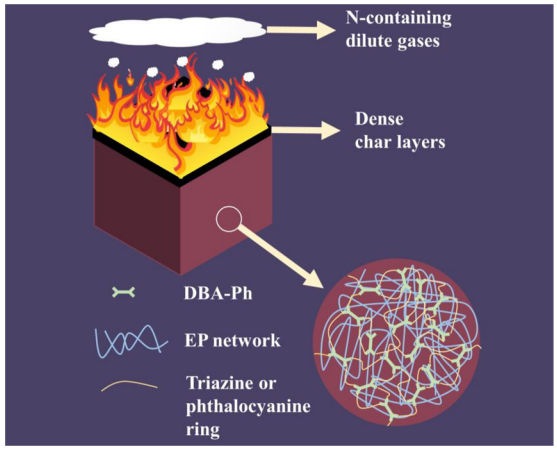

Figure 13. Flame retardant mechanism of DBA-Ph.

4. CONCLUSION

In this paper, a phosphorus-free cross-linked flame retardant had been successfully prepared. And after introducing it into EP thermosets, a simple thermal treatment procedure was applied to make the DBA-Ph cross-link inside the EP network. And with only 10 wt % DBA-Ph, the samples reached a UL-94 V-0 rate; when the content raises to 20 wt %, the modified samples can reach an LOI value of 34.9% and lower the PHRR value 40.1% compared with pure EP. The residue char and gas products analyses have proved that the flame retardant has both condensed phase and gas phase flame-retardant effects; besides the excellent flame-retardant properties, the phosphorus-free compounds can solve the toxic gas release problem.

https://doi.org/10.1021/acsomega.2c03167
ACS Omega 2022, 7, 37170−37179

AUTHOR INFORMATION

Corresponding Authors

Penglun Zheng − *College of Civil Aviation Safety Engineering, Civil Aviation Flight University of China, Guanghan 618307, China; Civil Aircraft Fire Science and Safety Engineering Key Laboratory of Sichuan Province, Deyang, Sichuan 618307, China;* orcid.org/0000-0002-8081-2636; Email: 18482179228@163.com

Xue Li − *School of Mechanical Engineering, Beijing Institute of Technology, Beijing 100081, China*; Email: lixue@bit.edu.cn

Quanyi Liu − *College of Civil Aviation Safety Engineering, Civil Aviation Flight University of China, Guanghan 618307, China; Civil Aircraft Fire Science and Safety Engineering Key Laboratory of Sichuan Province, Deyang, Sichuan 618307, China*; Email: quanyiliu2005@cafuc.edu.cn

Authors

Rui Wang − *College of Civil Aviation Safety Engineering, Civil Aviation Flight University of China, Guanghan 618307, China; Civil Aircraft Fire Science and Safety Engineering Key Laboratory of Sichuan Province, Deyang, Sichuan 618307, China*

Junwei Li − *College of Civil Aviation Safety Engineering, Civil Aviation Flight University of China, Guanghan 618307, China; Civil Aircraft Fire Science and Safety Engineering Key Laboratory of Sichuan Province, Deyang, Sichuan 618307, China*

Jichang Sun − *College of Civil Aviation Safety Engineering, Civil Aviation Flight University of China, Guanghan 618307, China; Civil Aircraft Fire Science and Safety Engineering Key Laboratory of Sichuan Province, Deyang, Sichuan 618307, China*

Huaiyin Liu − *College of Civil Aviation Safety Engineering, Civil Aviation Flight University of China, Guanghan 618307, China; Civil Aircraft Fire Science and Safety Engineering Key Laboratory of Sichuan Province, Deyang, Sichuan 618307, China*

Complete contact information is available at: https://pubs.acs.org/10.1021/acsomega.2c03167

Author Contributions

R.W.: investigation, data curation, writing—original draft. P.Z.: supervision, funding acquisition. J.L.: formal analysis, writing—review and editing. J.S.: Methodology, review. H.L.: Supervision, methodology. X.L.: Supervision. Q.L.: Supervision, funding acquisition.

Notes

The authors declare no competing financial interest.

ACKNOWLEDGMENTS

The authors greatly appreciate the funding support of National Natural Science Foundation of China (Grant No. U2033206), Civil Aviation Flight University of China (Grant No. J2021-110, J2020-111), and Civil Aviation Flight University of China Graduate Innovation Program (XSY2022-05).

REFERENCES

(1) Teng, N.; Dai, J.; Wang, S.; Hu, J.; Liu, X. Hyperbranched flame retardant for epoxy resin modification: Simultaneously improved flame retardancy, toughness and strength as well as glass transition temperature. *Chem. Eng. J.* **2022**, *428*, 131226−131237.

(2) Peng, X.; Li, Z.; Wang, D.; Li, Z.; Liu, C.; Wang, R.; Jiang, L.; Liu, Q.; Zheng, P. A facile crosslinking strategy endows the traditional additive flame retardant with enormous flame retardancy improvement. *Chem. Eng. J.* **2021**, *424*, 130404−130419.

(3) Jia, K.; Zhao, R.; Zhong, J.; Liu, X. Preparation and characterization of iron phthalocyanine polymer magnetic materials. *J. Mater. Sci. Mater. Electron* **2010**, *21*, 708−712.

(4) Tenreiro Machado, J. A.; Lopes, A. M.; de Camposinhos, R. Fractional-order modelling of epoxy resin. *Philos. Trans. R. Soc. A* **2020**, *378*, 20190292.

(5) Cheng, J.; Wang, J.; Yang, S.; Zhang, Q.; Hu, Y.; Ding, G.; Huo, S. Aminobenzothiazole-substituted cyclotriphosphazene derivative as reactive flame retardant for epoxy resin. *React. Funct. Polym.* **2020**, *146*, 104412−104421.

(6) Huo, S.; Yang, S.; Wang, J.; Cheng, J.; Zhang, Q.; Hu, Y.; Ding, G.; Zhang, Q.; Song, P. A liquid phosphorus-containing imidazole derivative as flame-retardant curing agent for epoxy resin with enhanced thermal latency, mechanical, and flame-retardant performances. *J. Hazard. Mater.* **2020**, *386*, 121984−122012.

(7) Guo, W.; Wang, X.; Huang, J.; Cai, W.; Song, L.; Hu, Y. Intrinsically anti-flammable and self-toughened phosphorylated cardanol-derived novolac epoxy thermosets. *Ind. Crops. Prod.* **2021**, *166*, 113496−113508.

(8) Zhang, J.; Mi, X.; Chen, S.; Xu, Z.; Zhang, D.; Miao, M.; Wang, J. A bio-based hyperbranched flame retardant for epoxy resins. *Chem. Eng. J.* **2020**, *381*, 122719−122733.

(9) Dagdag, O.; Hsissou, R.; El Harfi, A.; Berisha, A.; Safi, Z.; Verma, C.; Ebenso, E.E.; Ebn Touhami, M.; El Gouri, M. Fabrication of polymer based epoxy resin as effective anti-corrosive coating for steel: Computational modeling reinforced experimental studies. *Surf. Interfaces.* **2020**, *18*, 100454−100466.

(10) Kamalipour, J.; Beheshty, M. H.; Jalaledin, M. Flame Retardant Compounds for Epoxy Resins: A Review. *Iran. J. Polym. Sci. Technol.* **2021**, *34*, 23−27.

(11) Huo, S.; Song, P.; Yu, B.; Ran, S.; Chevali, V. S.; Liu, L.; Fang, Z.; Wang, H. Phosphorus-containing flame retardant epoxy thermosets: recent advances and future perspectives. *Prog. Polym. Sci.* **2021**, *114*, 101366−101402.

(12) Dagdag, O.; Bachiri, A. E.; Hamed, O.; Haldhar, R.; Verma, C.; Ebenso, E.; Gouri, M. E. Dendrimeric Epoxy Resins Based on Hexachlorocyclotriphosphazene as a Reactive Flame Retardant Polymeric Materials: A Review. *J. Inorg. Organomet. Polym. Mater.* **2021**, *31*, 3240−3261.

(13) Yang, S.; Wang, J.; Huo, S.; Wang, M.; Cheng, L. Synthesis of a phosphorus/nitrogen-containing additive with multifunctional groups and its flame-retardant effect in epoxy resin. *Ind. Eng. Chem. Res.* **2015**, *54*, 7777−7786.

(14) Sun, Z.; Hou, Y.; Hu, Y.; Hu, W. Effect of additive phosphorus-nitrogen containing flame retardant on char formation and flame retardancy of epoxy resin. *Mater. Chem. Phys.* **2018**, *214*, 154−164.

(15) Leu, T.; Wang, C. Synergistic effect of a phosphorus−nitrogen flame retardant on engineering plastics. *J. Appl. Polym. Sci.* **2004**, *92*, 410−417.

(16) Huo, S.; Wang, J.; Yang, S.; Wang, J.; Zhang, B.; Zhang, B.; Chen, X.; Tang, Y. Synthesis of a novel phosphorus-nitrogen type flame retardant composed of maleimide, triazine-trione, and phosphaphenanthrene and its flame retardant effect on epoxy resin. *Polym. Degrad. Stab.* **2016**, *131*, 106−113.

(17) Yang, S.; Hu, Y.; Zhang, Q. Synthesis of a phosphorus−nitrogen-containing flame retardant and its application in epoxy resin. *High. Perform. Polym.* **2019**, *31*, 186−196.

(18) Wang, H.; Li, S.; Zhu, Z.; Yin, X.; Wang, L.; Weng, Y.; Wang, X. A novel DOPO-based flame retardant containing benzimidazolone structure with high charring ability towards low flammability and smoke epoxy resins. *Polym. Degrad. Stab.* **2021**, *183*, 109426−109456.

(19) Fang, M.; Qian, J.; Wang, X.; Chen, Z.; Guo, R.; Shi, Y. Synthesis of a Novel Flame Retardant Containing Phosphorus, Nitrogen, and Silicon and Its Application in Epoxy Resin. *ACS. Omega.* **2021**, *6*, 7094−7105.

(20) Cao, J.; Duan, H.; Zou, J.; Zhang, J.; Ma, H. A bio-based phosphorus-containing co-curing agent towards excellent flame retardance and mechanical properties of epoxy resin. *Polym. Degrad. Stab.* **2021**, *187*, 109548−109561.
(21) Akbari, V.; Jouyandeh, M.; Paran, S. M. R.; Ganjali, M. R.; Abdollahi, H.; Vahabi, H.; Ahmadi, Z.; Formela, K.; Esmaeili, A.; Mohaddespour, A.; Habibzadeh, S.; Saeb, M. Effect of Surface Treatment of Halloysite Nanotubes (HNTs) on the kinetics of epoxy resin cure with amines. *Polymers.* **2020**, *12*, 930−949.
(22) Meng, W.; Wu, H.; Bi, X.; Huo, Z.; Wu, J.; Jiao, Y.; Xu, J.; Wang, M.; Qu, H. Synthesis of ZIF-8 with encapsulated hexachlorocyclotriphosphazene and its quenching mechanism for flame-retardant epoxy resin. Microporous. *Mesoporous. Mater.* **2021**, *314*, 110885−110896.
(23) Liang, D.; Zhu, X.; Dai, P.; Lu, X.; Guo, H.; Que, H.; Wang, D.; He, T.; Xu, C.; Robin, H. M.; Luo, Z.; Gu, X. Preparation of a novel lignin-based flame retardant for epoxy resin. *Mater. Chem. Phys.* **2021**, *259*, 124101−124114.
(24) Araby, S.; Philips, B.; Meng, Q.; Ma, J.; Laoui, T.; Wang, C. Recent advances in carbon-based nanomaterials for flame retardant polymers and composites. *Compos. Part B Eng.* **2021**, *212*, 108675−108704.
(25) Zhang, A.; Zhao, H.; Cheng, J.; Li, M.; Li, S.; Cao, M.; Wang, Y. Construction of durable eco-friendly biomass-based flame-retardant coating for cotton fabrics. *Chem. Eng. J.* **2021**, *410*, 128361−128371.
(26) Wang, D.; Song, L.; Zhou, K.; Yu, X.; Hu, Y.; Wang, J. Anomalous nano-barrier effects of ultrathin molybdenum disulfide nanosheets for improving the flame retardance of polymer nanocomposites. *J. Mater. Chem. A* **2015**, *3*, 14307−14317.
(27) Jin, S.; Liu, Z.; Qian, L.; Qiu, Y.; Chen, Y.; Xu, B. Epoxy thermoset with enhanced flame retardancy and physical-mechanical properties based on reactive phosphaphenanthrene compound. *Polym. Degrad. Stab.* **2020**, *172*, 109063−109072.
(28) Yang, R.; Wei, R.; Li, K.; Tong, L.; Jia, K.; Liu, X. Crosslinked polyarylene ether nitrile film as flexible dielectric materials with ultrahigh thermal stability. *Sci. Rep.* **2016**, *6*, 36434.
(29) Tong, L.; Wei, R.; You, Y.; Liu, X. Post Self-crosslinking of phthalonitrile-terminated polyarylene ether nitrile crystals. *Polymers.* **2018**, *10*, 640−651.
(30) Zou, X.; Xu, M.; Jia, K.; Liu, X. Synthesis, polymerization, and properties of the allyl-functional phthalonitrile. *J. Appl. Polym. Sci.* **2014**, *131*, 41203−41210.
(31) Peng, X.; Liu, Q.; Wang, D.; Liu, C.; Zhao, Y.; Wang, R.; Zheng, P. A hyperbranched structure formed by in-situ crosslinking of additive flame retardant endows epoxy resins with great flame retardancy improvement. *Compos. Part. B. Eng.* **2021**, *224*, 109162−109177.
(32) Sun, J.; Wang, X.; Wu, D. Novel spirocyclic phosphazene-based epoxy resin for halogen-free fire resistance: synthesis, curing behaviors, and flammability characteristics. *ACS. Appl. Mater. Interfaces.* **2012**, *4*, 4047−4061.
(33) Wang, Y.; Yuan, Y.; Zhao, Y.; Liu, S.; Zhao, J. Flame−retarded epoxy resin with high glass transition temperature cured by DOPO-containing *H* -benzimidazole. *High. Perform. Polym.* **2017**, *29*, 94−103.
(34) Chen, Y.; Duan, H.; Ji, S.; Ma, H. Novel phosphorus/nitrogen/boron-containing carboxylic acid as co-curing agent for fire safety of epoxy resin with enhanced mechanical properties. *J. Hazard. Mater.* **2021**, *402*, 123769−123781.
(35) Wang, P.; Cai, Z. Highly efficient flame-retardant epoxy resin with a novel DOPO-based triazole compound: Thermal stability, flame retardancy and mechanism. *Polym. Degrad. Stab.* **2017**, *137*, 138−150.
(36) Zhang, Y.; Yan, H.; Feng, G.; Liu, R.; Yang, K.; Feng, W.; Zhang, S.; He, C. Non-aromatic Si, P, N-containing hyperbranched flame retardant on reducing fire hazards of epoxy resin with desirable mechanical properties and lower curing temperature. *Compos. Part. B. Eng.* **2021**, *222*, 109043−109055.
(37) Li, S.; Liu, Y.; Liu, Y.; Wang, Q. Synergistic effect of piperazine pyrophosphate and epoxy-octavinyl silsesquioxane on flame retardancy and mechanical properties of epoxy resin. *Compos. Part. B* **2021**, *223*, 109115−109127.
(38) Wang, P.; Chen, L.; Xiao, H.; Zhan, T. Nitrogen/sulfur-containing DOPO based oligomer for highly efficient flame-retardant epoxy resin. *Polym. Degrad. Stab.* **2020**, *171*, 109023−109055.
(39) Wu, J.; Chen, L.; Fu, T.; Zhao, H.; Guo, D.; Wang, X.; Wang, Y. New application for aromatic Schiff base: High efficient flame-retardant and anti-dripping action for polyesters. *Chem. Eng. J.* **2018**, *336*, 622−632.
(40) Xu, B.; Wu, X.; Ma, W.; Qian, L.; Xin, F.; Qiu, Y. Synthesis and characterization of a novel organic-inorganic hybrid char-forming agent and its flame-retardant application in polypropylene composites. *J. Anal. Appl. Pyrolysis.* **2018**, *134*, 231−242.
(41) Mao, M.; Yu, K.-X.; Cao, C.-F.; Gong, L.-X.; Zhang, G.-D.; Zhao, L.; Song, P.; Gao, J.-F.; Tang, L.-C. Facile and green fabrication of flame-retardant Ti3C2Tx MXene networks for ultrafast, reusable and weather-resistant fire warning. *Chem. Eng. J.* **2022**, *427*, 131615−131626.
(42) Zhang, Z.-H.; Chen, Z.-Y.; Tang, Y.-H.; Li, Y.-T.; Ma, D.; Zhang, G.-D.; Boukherroub, R.; Cao, C.-F.; Gong, L.-X.; Song, P.; Cao, K.; Tang, L.-C. Silicone/graphene oxide co-cross-linked aerogels with wide-temperature mechanical flexibility, super-hydrophobicity and flame resistance for exceptional thermal insulation and oil/water separation. *J. Mater. Sci. Technol.* **2022**, *114*, 131−142.
(43) Li, Y.; Liu, W.; Shen, F.; Zhang, G.; Gong, L.; Zhao, L.; Song, P.; Gao, J.; Tang, L. Processing, thermal conductivity and flame retardant properties of silicone rubber filled with different geometries of thermally conductive fillers: A comparative study. *Compos. Part. B* **2022**, *238*, 109907−109918.

https://doi.org/10.1021/acsomega.2c03167
ACS Omega 2022, 7, 37170−37179